Mathematical Biosciences and Engineering

http://www.aimspress.com/journal/MBE

Mathematical Biosciences and Engineering, 16(1): 474–500.
DOI: 10.3934/mbe.2019022
Received: 04 March 2018
Accepted: 13 September 2018
Published: 18 December 2018

Research article

Modelling and analysis of HFMD with the effects of vaccination, contaminated environments and quarantine in mainland China

Lei Shi[1,2], **Hongyong Zhao**[1,*] **and Daiyong Wu**[1,3]

[1] Department of Mathematics, Nanjing University of Aeronautics and Astronautics, Nanjing, 210016, China

[2] Department of Mathematics, Honghe University, Mengzi 661199, China

[3] Department of Mathematics, Anqing Normal University, Anqing 246133, China

* **Correspondence:** Email: hyzhao1967@126.com.

Abstract: Currently, hand, foot, and mouth disease (HFMD) is widespread in mainland China and seriously endangers the health of infants and young children. Recently in mainland China, preventing the spread of the disease has entailed vaccination, isolation measures, and virus clean-up in the contaminated environment. However, quantifying and evaluating the efficacy of these strategies on HFMD remains challenging, especially because relatively little research analyses the impact of EV71 vaccination for this disease. To assess the effectiveness of these strategies, we propose a new mathematical model that considers vaccination, contaminated environment, and quarantine simultaneously. Unlike the previous studies for HFMD, in which the basic reproduction number R_0 is the only threshold to decide whether the disease is extinct or not, our results show that another threshold value is needed: $\hat{R}_0 < 1$ ($R_0 \leq \hat{R}_0 < 1$) such that disease is extinct; i.e., the disease-free equilibrium is globally asymptotically stable. Moreover, numerical experiments show that our model may have positive equilibriums even if the basic reproduction number R_0 is less than 1. In designing a new algorithm based on a BP network to estimate the unknown parameters, this proposed model is put forward to individually fit the HFMD reported cases annually in mainland China from 2015 to 2017. At last, the sensitivity analyses and numerical experiments show that increasing the rate of virus clearance, the vaccinated rate of infants and young children, and the quarantined rate of infectious individuals can effectively control the spread of HFMD in mainland China. Nevertheless, it remains difficult to eliminate the disease. Specifically, our results show that the current vaccine measures starting in 2016 have reduced the total number of patients in 2016 and 2017 by 17% and 22%, respectively.

Keywords: HFMD; vaccination; BP network; basic reproduction number; contaminated environment; quarantine

1. Introduction

Hand, foot, and mouth disease (HFMD) is a common childhood illness, mainly caused by coxsackievirus A16 (CVA16) and enterovirus 71 (EV71), as well as certain enteroviruses, including coxsackievirus A4, 5, 9, 10, B2 and 5 [1, 2]. HFMD usually occurs in children under six years old, although it may also occur in older children and adults [3]. The usual incubation period is 2 to 7 days, and an infected individual will fully recover after 2 to 10 days. HFMD was first reported in New Zealand in 1957 and first named in America in 1959 [4], then it has widely spread in America [5], Europe [6, 7] and Asia [8, 9, 10, 11, 12, 13, 14, 15, 16, 17].

Recently, HFMD has seriously threatened the health of infants and young children in mainland China. It has been classified as a class III infectious disease in the National Stationary Notifiable Communicable Diseases, and the annual data of HFMD have been archived by the Chinese Center for Disease Control and Prevention (CCDC) [3] and the National Health and Family Planning Commission of the People's Republic of China (NHFPC) [18] since 2008. Figure 1 shows the reported annual cumulative cases of more than 1.5 million since 2010 and more than 2 million since 2014. In analyses of analyze the epidemiological characteristics and pathogenic spectrum of FHMD in mainland China, EV71 and CVA16 have been considered major pathogens in the past decade, and the positive rates of EV71 and CVA16 were about 35%∼55% and 20%∼35%, respectively [19, 20, 21, 22, 23]. As described in [22, 23], the EV71 vaccine was developed and has been used in mainland China since 2016, which have protected many young children protect away from the EV71 virus infections. And, from the data shown in Figure 1, we conclude that vaccination measures may have led to a lower number of cases in 2016 or 2017 than in 2014 or 2015, in contrast to the diseases trend in the past. The clinical trial results [22, 23] showed that the vaccine provides immunity only for the EV71 virus; it provides no form of protection against infection for other viruses. Furthermore, there are few studies on the effects of EV71 vaccination on the spread of HFMD. It should be noted that epidemiological modelling is an important tool helpful to understand infectious disease spread and control [24, 25, 26].

A number of epidemiological models that do not consider EV71 vaccination have been established to investigate the transmission dynamics and to predict infections of HFMD. For instance, Wang and Sung (2006) [27] used a susceptible-infectious-recovered (SIR) model to analyse epidemic situations of FHMD in Taiwan from 1999 to 2003; Tiing and Labadin (2008) [28] studied SIR model to predict the number of the infected and the duration of an outbreak in Sarawak Malaysia; Roy and Halder (2012) [29] proposed a susceptible-exposed-infectious-quarantine-recovered ($SEIQR$) model of HFMD; Ma and Liu (2013) [30] extended the $SEIQR$ model, considered asymptomatic infectious, to formulate a more realistic $SEII_eR$ model, which has been fitted to data of HFMD in Shandong Province, China; Wang and Xiao (2016) [31, 32] further considered indirect transmission coming from the contaminated environment to establish an $SEII_eRW$ model. Moreover, some studies on the dynamical behaviors or application of the above models are shown in [33, 34, 35, 36, 37, 38, 39, 40]. However, most of these models have considered either quarantine for infectious individuals [30, 35, 37] or contaminated environment caused by infectious individuals [31] alone. Moreover, no previous studies have considered the shared effects of vaccination, quarantine measures, and maintaining sanitation on disease. From the point view of practical application, the lack of key factors may affect the modeling.

To quantify these issues, we propose a new mathematical model, which extends the existing ones

such as $SEIQR$ [30] and $SEII_eRW$ [31], to analyse the effects of EV71 vaccination, clean-up of contaminated environments, and quarantine on HFMD in mainland China simultaneously. In order to analyse the effects of EV71 vaccination, we take the individuals withEV71 vaccination as an independent compartment in modelling, which is a well deal with the case that EV71 vaccine against the EV71 virus but not against others. A combination of analytical and numerical techniques are used to analyze the proposed model. Finally, we use our model to individually fit the monthly reported data of HFMD in mainland China from 2015 to 2017. This paper is organized as follows: In Section 2, a novel epidemiological model of HFMD is proposed. In Section 3, the dynamic behaviors of this model are analyzed. In Section 4, the model is used to fit the real reported data, and some control strategies are discussed. In Section 5, we discuss and summarize our conclusions. In Appendix A, a new estimating algorithm based on BP neural network is designed.

2. Model formulation

In this section, we propose an eight-compartment HFMD model, named $SVEII_eQRW$. The underlying structure of the model comprises classes of individuals are susceptible $S(t)$, vaccinated $V(t)$ (individuals with EV71 vaccine), exposed but not yet infectious $E(t)$, infectious with symptoms (symptomatic infectious) $I(t)$, infectious but not yet symptomatic (asymptomatic infectious) $I_e(t)$, infectious and hospitalized or quarantined or isolated $Q(t)$, and recovered $R(t)$. Using the same description in [31], $W(t)$ is the density of pathogen of the contaminated environment including door handles, towels, handkerchiefs, toys, utensils, bedding, underclothes, etc. at time t. Note that the individuals $V(t)$ vaccinated with EV71 vaccine can also be infected with FHMD by FHMD viruses except EV71.

A flow diagram describing the model is shown in Figure 2, and the model can be represented by the following ordinary differential equations:

$$\begin{cases} \dfrac{dS}{dt} = \Lambda - \beta_1 SI - \beta_2 SI_e - \sigma SW - kS - dS + \eta_1 R, \\ \dfrac{dV}{dt} = kS - \bar{\beta}_1 VI - \bar{\beta}_2 VI_e - \bar{\sigma} VW - dV + \eta_2 R, \\ \dfrac{dE}{dt} = \beta_1 SI + \beta_2 SI_e + \sigma SW + \bar{\beta}_1 VI + \bar{\beta}_2 VI_e + \bar{\sigma} VW - \alpha E - dE, \\ \dfrac{dI}{dt} = \alpha\rho E - pI - \gamma_1 I - dI - mI, \\ \dfrac{dI_e}{dt} = \alpha(1-\rho)E - \gamma_3 I_e - dI_e, \\ \dfrac{dQ}{dt} = pI - \gamma_2 Q - dQ - mQ, \\ \dfrac{dR}{dt} = \gamma_1 I + \gamma_2 Q + \gamma_3 I_e - \eta_1 R - \eta_2 R - dR, \\ \dfrac{dW}{dt} = \lambda_1 I + \lambda_2 I_e - \delta W, \end{cases} \tag{2.1}$$

where k, p are nonnegative, other parameters are positive and its biological meanings are listed in Table 1.

Remark 1. Only the authors in [32] have considered the vaccination measure for HFMD, but it assumed that vaccinees against all HFMD viruses, in which the individuals being vaccinated in the susceptible class straight enter to the recovered class in modelling. However, it should be noted that the current vaccine is only resistant to the EV71 virus [22, 23], which is well modeled in our model by adding a vaccinated class $V(t)$. In addition, the previous studies did not have taken into account the effects of both contaminated environment and quarantine on the spread of disease.

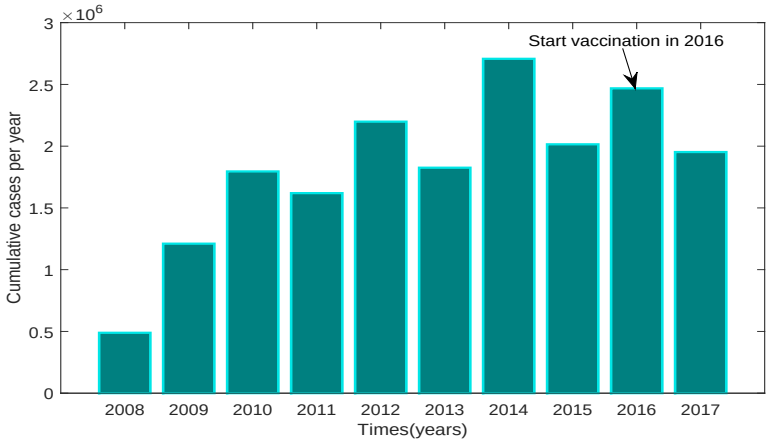

Figure 1. The annual cumulative cases of HFMD from the Chinese Center for Disease Control and Prevention (CCDC) [3] and the National Health and Family Planning Commission of the Peoples Republic of mainland China (NHFPC) [18].

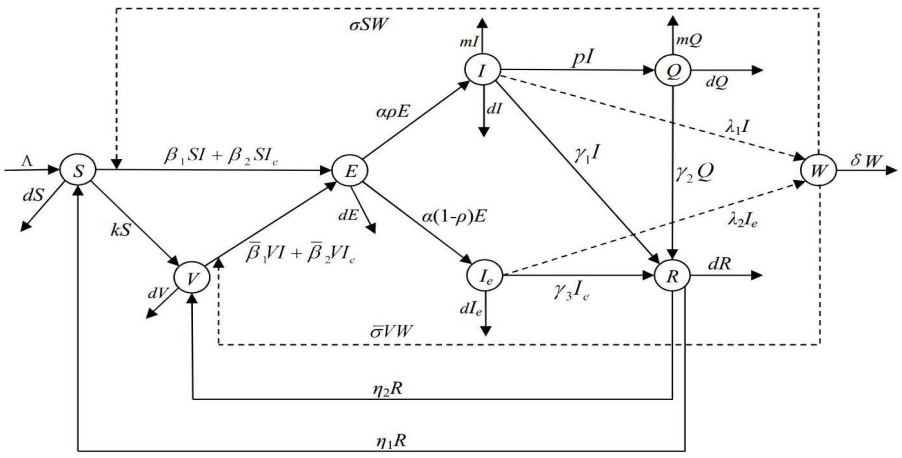

Figure 2. Flow diagram represents transmission routes and other processes modeled by system (2.1).

3. Stability analysis and persistence

In this section, we discuss the dynamic behaviors for system (2.1). We first introduce some notations which will be used throughout this paper. $\mathbb{R}^n$ denotes the n-dimensional Euclidean space, and $\mathbb{R}^n_+ \triangleq \{(x_1, x_2, \cdots, x_n) \in \mathbb{R}^n : x_i \geq 0, i = 1, \cdots, n\}$. $A = (a_{ij})_{n\times n}$ denotes a matrix of $n \times n$ real matrices.

Table 1. Parameter definition of HFMD model.

Parameter	Definition
Λ	Recruitment rate
β_1, β_2, and σ	Transmission rate from $I(t)$, $I_e(t)$, and $W(t)$ to $S(t)$ respectively
$\bar{\beta}_1, \bar{\beta}_2$, and $\bar{\sigma}$	Transmission rate from $I(t)$, $I_e(t)$, and $W(t)$ to $V(t)$ respectively
m	Disease-related death of HFMD
d	Progression rate leaving the children group below the age of six
k	Vaccinated rate of $S(t)$
η_1 and η_2	Rate from $R(t)$ to $S(t)$ and $V(t)$ respectively
$1/\alpha$	Average incubation period
ρ	Proportion of symptomatic infectious individuals
γ_1, γ_2, and γ_3	Recovery rate of $I(t)$, $I_e(t)$, and $Q(t)$ respectively
p	Quarantine rate at which symptomatic infectious individuals $I(t)$ enters into quarantine individuals $Q(t)$
λ_1 and λ_2	Virus shedding rate from symptomatic and asymptomatic infected individuals respectively
δ	Clearance rate of pathogens $W(t)$

The superscript T denotes matrix or vector transposition. For a continuous and bounded function $f : [0, +\infty) \to R$, denote $f_\infty = \liminf_{t\to+\infty} f(t)$ and $f^\infty = \limsup_{t\to+\infty} f(t)$. Let

$$\varphi(0) = (S(0), V(0), E(0), I(0), I_e(0), Q(0), R(0), W(0)) \in \mathbb{R}^8_+$$

be the initial condition of system (2.1). Clearly, any solution of system (2.1) with non-negative initial conditions is non-negative, and the following lemma shows that the solutions are uniformly ultimately bounded.

Lemma 3.1. *The solutions of system (2.1) eventually enter*

$$\begin{aligned}\Gamma =&\{(S(t), V(t), E(t), I(t), I_e(t), Q(t), R(t), W(t)) \in \mathbb{R}^8_+ : 0 \le S(t) + V(t)\\ &+ E(t) + I(t) + I_e(t) + Q(t) + R(t) \le \frac{\Lambda}{d}, 0 \le W(t) \le \frac{(\lambda_1 + \lambda_2)\Lambda}{d\delta}\}.\end{aligned}$$

Proof. It is obvious that the population size $N(t) = S(t) + V(t) + E(t) + I(t) + I_e(t) + Q(t) + R(t) \ge 0$ and $W(t) \ge 0$. From system (2.1), the population size satisfies the following equation

$$\begin{aligned}\frac{dN}{dt} &= \Lambda - dS - dV - dE - dI - dI_e - (d+m)Q - (d+\mu)R\\ &= \Lambda - dN - m(I+Q)\\ &\le \Lambda - dN. \end{aligned} \tag{3.1}$$

According to the comparison theorem, there exists $t_1 > 0$ such that $N(t) \le \frac{\Lambda}{d}$, for $t \ge t_1$.

It follows from the last equation of (2.1) that for $t \ge t_1$,

$$\begin{aligned}\frac{dW}{dt} &= \lambda_1 I + \lambda_2 I_e - \delta W\\ &\le (\lambda_1 + \lambda_2)N - \delta W\\ &\le (\lambda_1 + \lambda_2)\frac{\Lambda}{d} - \delta W. \end{aligned} \tag{3.2}$$

Similarly, there exists $t_2 > t_1$ such that $W(t) \le \frac{(\lambda_1+\lambda_2)\Lambda}{d\delta}$, for $t \ge t_2$. Therefore, the solutions of system (2.1) are uniformly ultimately bounded. This completes the proof. □

It is clear that system (2.1) has a disease-free equilibrium

$$E_0(S^0, V^0, E^0, I^0, I_e^0, Q^0, R^0, W^0) = (\frac{\Lambda}{k+d}, \frac{k\Lambda}{d(k+d)}, 0, 0, 0, 0, 0, 0).$$

Using the next generation matrix method developed by Van den and Watmough [41], we obtain the basic reproduction number

$$R_0 = R_1 + R_2 + R_3, \tag{3.3}$$

where

$$R_1 = \frac{\rho\alpha(\beta_1 S^0 + \bar{\beta}_1 V^0)}{(\alpha+d)(p+\gamma_1+d+m)} \triangleq \rho R_I,$$

$$R_2 = \frac{(1-\rho)\alpha(\beta_2 S^0 + \bar{\beta}_2 V^0)}{(\alpha+d)(\gamma_3+d)} \triangleq (1-\rho)R_{I_e},$$
$$R_3 = \left(\frac{\alpha\rho\lambda_1}{(\alpha+d)(p+\gamma_1+d+m)\delta} + \frac{\alpha(1-\rho)\lambda_2}{(\alpha+d)(\gamma_3+d)\delta}\right)(\sigma S^0 + \bar{\sigma} V^0),$$

and

$$R_I = \frac{\alpha(\beta_1 S^0 + \bar{\beta}_1 V^0)}{(\alpha+d)(p+\gamma_1+d+m)},$$
$$R_{I_e} = \frac{\alpha(\beta_2 S^0 + \bar{\beta}_2 V^0)}{(\alpha+d)(\gamma_3+d)}.$$

R_I is the average number of secondary infected individuals generated by a symptomatic infected individual; R_{I_e} is the average number of secondary infected individuals generated by an asymptomatic infected individual; R_3 is the average number of secondary infected individuals generated by free-living viruses in the environment shed by the infected individuals. R_0 is a central concept in measuring the transmission of infectious diseases.

In this following, we discuss the stability of the disease-free equilibrium and the persistence for system (2.1).

Theorem 3.2. *The disease-free equilibrium E_0 is locally asymptotically stable if $R_0 < 1$ and unstable if $R_0 > 1$.*

Proof. The Jacobian matrix $J(E_0)$ of system (2.1) at E_0 is given by

$$\begin{bmatrix}
-(k+d) & 0 & 0 & -\beta_1 S^0 & -\beta_2 S^0 & 0 & \eta_1 & -\sigma S^0 \\
k & -d & 0 & -\bar{\beta}_1 V^0 & -\bar{\beta}_2 V^0 & 0 & \eta_2 & -\bar{\sigma} V^0 \\
0 & 0 & -(\alpha+d) & \beta_1 S^0 + \bar{\beta}_1 V^0 & \beta_2 S^0 + \bar{\beta}_2 V^0 & 0 & 0 & \sigma S^0 + \bar{\sigma} V^0 \\
0 & 0 & \alpha\rho & -(p+\gamma_1+d+m) & 0 & 0 & 0 & 0 \\
0 & 0 & \alpha(1-\rho) & 0 & -(\gamma_3+d) & 0 & 0 & 0 \\
0 & 0 & 0 & p & 0 & -(\gamma_2+d+m) & 0 & 0 \\
0 & 0 & 0 & \gamma_1 & \gamma_3 & \gamma_2 & -(\eta_1+\eta_2+d) & 0 \\
0 & 0 & 0 & \lambda_1 & \lambda_2 & 0 & 0 & -\delta
\end{bmatrix}. \tag{3.4}$$

We can obtain the eigenvalues for (3.4) as $-(k+d)$, $-d$, $-(\gamma_2+d+m)$, $-(\eta_1+\eta_2+d)$, and roots of

$$\lambda^4 + a_1\lambda^3 + a_2\lambda^2 + a_3\lambda + a_4 = 0, \tag{3.5}$$

where

$$\begin{aligned}
a_1 &= (\alpha+d) + (p+\gamma_1+d+m) + (\gamma_3+d), \\
a_2 &= (\alpha+d)\delta + (p+\gamma_1+d+m)(\gamma_3+d) + (\gamma_3+d)\delta \\
&\quad + (\alpha+d)(p+\gamma_1+d+m)(1-R_1) + (\alpha+d)(\gamma_3+d)(1-R_2), \\
a_3 &= (p+\gamma_1+d+m)(\gamma_3+d)\delta + (\alpha+d)(p+\gamma_1+d+m)[1-(R_1+R_2)] \\
&\quad + (\alpha+d)(p+\gamma_1+d+m)(\gamma_3+d)\delta(1-R_3), \\
a_4 &= (\alpha+d)(p+\gamma_1+d+m)(\gamma_3+d)\delta(1-R_0).
\end{aligned}$$

Note that if $R_0 < 1$, then $R_1 < 1$, $R_2 < 1$, $R_3 < 1$. Hence, it can get that $a_i > 0, i = 1, \cdots, 4$. Further, one has

$$\begin{vmatrix} a_1 & 1 \\ a_3 & a_2 \end{vmatrix} > 0, \quad \begin{vmatrix} a_1 & 1 & 0 \\ a_3 & a_2 & a_1 \\ 0 & a_4 & a_3 \end{vmatrix} > 0, \quad \begin{vmatrix} a_1 & 1 & 0 & 0 \\ a_3 & a_2 & a_1 & 1 \\ 0 & a_4 & a_3 & a_2 \\ 0 & 0 & 0 & a_4 \end{vmatrix} > 0.$$

According to Hurwitz criterion, all the roots of (3.5) have negative real part. Therefore, E_0 is locally asymptotically stable. If $R_0 > 1$, then $a_4 < 0$. This means that (3.5) has at least one positive real part root. Then, E_0 is unstable. This completes the proof. □

In order to analyse the global asymptotic stability of the disease-free equilibrium E_0 for system (2.1), denote

$$\hat{R}_0 = \Big\{ \frac{\rho\alpha\hat{\beta}_1}{(\alpha+d)(p+\gamma_1+d+m)} + \frac{(1-\rho)\alpha\hat{\beta}_2}{(\alpha+d)(\gamma_3+d)} + \Big(\frac{\alpha\rho\lambda_1}{(\alpha+d)(p+\gamma_1+d+m)\delta} + \frac{\alpha(1-\rho)\lambda_2}{(\alpha+d)(\gamma_3+d)\delta} \Big)\hat{\sigma} \Big\} \frac{\Lambda}{d},$$

where $\hat{\beta}_1 = \max(\beta_1, \bar{\beta}_1), \hat{\beta}_2 = \max(\beta_2, \bar{\beta}_2), \hat{\sigma} = \max(\sigma, \bar{\sigma})$. It is obvious that $R_0 \le \hat{R}_0$. Moreover, it follows that $R_0 = \hat{R}_0$ if and only if $\beta_1 = \bar{\beta}_1, \beta_2 = \bar{\beta}_2, \sigma = \bar{\sigma}$.

Theorem 3.3. *If $\hat{R}_0 < 1$, then the disease-free equilibrium E_0 is globally asymptotically stable.*

Proof. From Theorem 3.2, we have that E_0 is locally asymptotically stable. Then, it only needs to prove the global attraction of the disease-free equilibrium E_0.

Note that any solution of system (2.1) with nonnegative initial is nonnegative and uniformly ultimataly bounded. By the fluctuation lemma [42], there exists a sequence $\{t_n\}$ such that $t_n \to +\infty, S(t_n) \to S^\infty$ and $\frac{dS(t_n)}{dt} \to 0$ as $n \to +\infty$. It follows from the first equation of (2.1) that

$$\begin{aligned} &\frac{dS(t_n)}{dt} + \beta_1 S(t_n) I(t_n) + \beta_2 S(t_n) I_e(t_n) + \sigma S(t_n) W(t_n) + (k+d) S(t_n) \\ &= \Lambda + \eta_1 R(t_n). \end{aligned} \tag{3.6}$$

Letting $n \to +\infty$, one has from (3.6) that

$$(k+d) S^\infty \le [(k+d) + I_\infty + I_{e\infty} + W_\infty] S^\infty \le \Lambda + \eta_1 R^\infty. \tag{3.7}$$

Similarly, it follows from the other equations of (2.1) that

$$dV^\infty \le (d + I_\infty + I_{e\infty} + W_\infty) V^\infty \le k S^\infty + \eta_2 R^\infty, \tag{3.8}$$

$$(\alpha+d) E^\infty \le (\beta_1 I^\infty + \beta_2 I_e^\infty + \sigma W^\infty) S^\infty + (\bar{\beta}_1 I^\infty + \bar{\beta}_2 I_e^\infty + \bar{\sigma} W^\infty) V^\infty, \tag{3.9}$$

$$(p+\gamma_1+d+m) I^\infty \le \alpha\rho E^\infty, \tag{3.10}$$

$$(\gamma_3+d) I_e^\infty \le \alpha(1-\rho) E^\infty, \tag{3.11}$$

$$(\gamma_2+d+m) Q^\infty \le p I^\infty, \tag{3.12}$$

$$(\eta_1+\eta_2+d) R^\infty \le \gamma_1 I^\infty + \gamma_2 Q^\infty + \gamma_3 I_e^\infty, \tag{3.13}$$

$$\delta W^{\infty} \leq \lambda_1 I^{\infty} + \lambda_2 I_e^{\infty}. \tag{3.14}$$

By (3.7) and (3.8), one has

$$S^{\infty} \leq \frac{\Lambda}{k+d} + \frac{\eta_1}{k+d} R^{\infty}, \tag{3.15}$$

$$V^{\infty} \leq \frac{k\Lambda}{d(k+d)} + \frac{k\eta_1}{d(k+d)} R^{\infty} + \frac{\eta_2}{d} R^{\infty}. \tag{3.16}$$

We claim that $E^{\infty} = 0$. Suppose not, it follows from (3.10), (3.11) and (3.14) that

$$I^{\infty} \leq \frac{\alpha\rho}{p+\gamma_1+d+m} E^{\infty}, \tag{3.17}$$

$$I_e^{\infty} \leq \frac{\alpha(1-\rho)}{\gamma_3+d} E^{\infty}, \tag{3.18}$$

$$W^{\infty} \leq \frac{\lambda_1\alpha\rho}{\delta(p+\gamma_1+d+m)} E^{\infty} + \frac{\lambda_2\alpha(1-\rho)}{\delta(\gamma_3+d)} E^{\infty}. \tag{3.19}$$

Substituting inequalities (3.17), (3.18), (3.19) into (3.9), after some simplification, we derive that

$$\begin{aligned} &\frac{\rho\alpha(\beta_1 S^{\infty} + \bar{\beta}_1 V^{\infty})}{(\alpha+d)(p+\gamma_1+d+m)} + \frac{(1-\rho)\alpha(\beta_2 S^{\infty} + \bar{\beta}_2 V^{\infty})}{(\alpha+d)(\gamma_3+d)} + \Big(\frac{\alpha\rho\lambda_1}{(\alpha+d)(p+\gamma_1+d+m)\delta} \\ &+ \frac{\alpha(1-\rho)\lambda_2}{(\alpha+d)(\gamma_3+d)\delta} \Big)(\sigma S^{\infty} + \bar{\sigma} V^{\infty}) \geq 1. \end{aligned} \tag{3.20}$$

By (3.20), one has that

$$\begin{aligned} &\Big\{ \frac{\rho\alpha\hat{\beta}_1}{(\alpha+d)(p+\gamma_1+d+m)} + \frac{(1-\rho)\alpha\hat{\beta}_2}{(\alpha+d)(\gamma_3+d)} + \Big(\frac{\alpha\rho\lambda_1}{(\alpha+d)(p+\gamma_1+d+m)\delta} + \\ &\frac{\alpha(1-\rho)\lambda_2}{(\alpha+d)(\gamma_3+d)\delta} \Big)\hat{\sigma} \Big\}(S^{\infty} + V^{\infty}) \\ &\geq \frac{\rho\alpha(\beta_1 S^{\infty} + \bar{\beta}_1 V^{\infty})}{(\alpha+d)(p+\gamma_1+d+m)} + \frac{(1-\rho)\alpha(\beta_2 S^{\infty} + \bar{\beta}_2 V^{\infty})}{(\alpha+d)(\gamma_3+d)} + \\ &\Big(\frac{\alpha\rho\lambda_1}{(\alpha+d)(p+\gamma_1+d+m)\delta} + \frac{\alpha(1-\rho)\lambda_2}{(\alpha+d)(\gamma_3+d)\delta} \Big)(\sigma S^{\infty} + \bar{\sigma} V^{\infty}) \geq 1. \end{aligned} \tag{3.21}$$

It follows from (3.21) that

$$S^{\infty} + V^{\infty} \geq \frac{\Lambda}{d\hat{R}_0},$$

which is a contradiction since $S^{\infty} + V^{\infty} \leq \frac{\Lambda}{d}$ and $\hat{R}_0 < 1$. This proves the claim. Since $E^{\infty} = 0$, then one has from (3.10)-(3.14) that $I^{\infty} = 0, I_e^{\infty} = 0, Q^{\infty} = 0, R^{\infty} = 0, W^{\infty} = 0$. Therefore,

$$\lim_{t\to+\infty} E(t) = \lim_{t\to+\infty} I(t) = \lim_{t\to+\infty} I_e(t) = \lim_{t\to+\infty} Q(t) = \lim_{t\to+\infty} R(t) = \lim_{t\to+\infty} W(t) = 0. \tag{3.22}$$

By (3.15) and (3.16), one has

$$S^{\infty} \leq \frac{\Lambda}{k+d}, V^{\infty} \leq \frac{k\Lambda}{d(k+d)}. \tag{3.23}$$

Moreover, using the fluctuation lemma again, there exists a sequence $\{s_n\}$ such that $s_n \to +\infty, S(s_n) \to +\infty$, and $\frac{dS(s_n)}{dt} \to 0$ as $n \to +\infty$. By the first and second equations of (2.1), one has

$$\begin{aligned}\frac{dS(s_n)}{dt} &= \Lambda - \beta_1 S(s_n)I(s_n) - \beta_2 S(s_n)I_e(s_n) - \sigma S(s_n)W(s_n) - (k+d)S(s_n)\\ &\quad + \eta_1 R(s_n),\\ \frac{dV(s_n)}{dt} &= kS(s_n) - \bar{\beta}_1 V(s_n)I(s_n) - \bar{\beta}_2 V(s_n)I_e(s_n) - \bar{\sigma} V(s_n)W(s_n) - dV(s_n)\\ &\quad + \eta_2 R(s_n).\end{aligned}$$

Letting $n \to +\infty$ and by using (3.22), we obtain that

$$S_\infty = \frac{\Lambda}{k+d}, V_\infty = \frac{k\Lambda}{d(k+d)}. \tag{3.24}$$

It follows from (3.23) and (3.24) that

$$\lim_{t\to+\infty} S(t) = \frac{\Lambda}{k+d}, \lim_{t\to+\infty} V(t) = \frac{k\Lambda}{d(k+d)}.$$

Thus,

$$\lim_{t\to+\infty} (S(t), V(t), E(t), I(t), I_e(t), Q(t), R(t), W(t)) = E_0.$$

This completes the proof. □

Theorem 3.4. *If $R_0 > 1$, then system (2.1) is uniformly persistent. That is, if $R_0 > 1$, there exists a small positive constant $\varepsilon > 0$ such that $I_\infty > \varepsilon$, $I_{e\infty} > \varepsilon$ for system (2.1) with initial value $\varphi(0)$ and $I(0) > 0$, $I_e(0) > 0$.*

Proof. In order to prove this result, the uniform persistence theorem in [44] is used. Define

$$\begin{aligned}&X = \{(S, V, E, I, I_e, Q, R, W) \in \Gamma\},\\ &X_0 = \{(S, V, E, I, I_e, Q, R, W) \in X : E > 0, I > 0, I_e > 0, Q > 0, R > 0, W > 0\},\\ &\partial X_0 = X \backslash X_0.\end{aligned}$$

Now we prove that system (2.1) is uniformly persistent with respect to (X, X_0).

First, it is easy to verify that both X and X_0 are positively invariant for system (2.1), and X_0 is relatively closed in X. Moreover, by Theorem 3.1, the system (2.1) is point dissipative. Thus, the system (2.1) must exist a globally attractor. Set

$$\begin{aligned}M_\partial = &\{(S(0), V(0), E(0), I(0), I_e(0), Q(0), R(0), W(0)) \in \partial X_0 : (S(t), V(t),\\ &E(t), I(t), I_e(t), Q(t), R(t), W(t)) \in \partial X_0, \forall t \geq 0\}.\end{aligned}$$

Now we prove that

$$M_\partial = \{(S, V, 0, 0, 0, 0, 0, 0) \in \partial X : S \geq 0, V \geq 0\} \triangleq M'_\partial.$$

It is obvious that $M'_\partial \subseteq M_\partial$, then we only need to prove $M_\partial \subseteq M'_\partial$. Suppose not, let $\varphi(t)$ be a solution of system (2.1) with the initial condition $\varphi(0)$. Then, for any

$$\varphi(t) = (S(t), V(t), E(t), I(t), I_e(t), Q(t), R(t), W(t)) \in M_\partial$$

and $\varphi(t) \neq M'_\partial$, there must exist at least one of $E(t)$, $I(t)$, $I_e(t)$, $Q(t)$, $R(t)$, $W(t)$ which is not zero. Without loss of generality, assume that $E(t) = 0$, $I(t) = 0$, $I_e(t) = 0$, $Q(t) = 0$, $R(t) = 0$, but $W(t) > 0$. From system (2.1), one has the following equations, for $\forall t > 0$,

$$\begin{aligned}
E(t) &= e^{-(\alpha+d)t}\Big[E(0) + \int_0^t [(\beta_1 I(u) + \beta_2 I_e(u) + \sigma W(u))S(u) \\
&\quad + (\bar{\beta}_1 I(u) + \bar{\beta}_2 I_e(u) + \bar{\sigma} W(u))V(u)]du\Big] > 0, \\
I(t) &= e^{-(p+\gamma_1+d+m)t}[I(0) + \int_0^t \alpha\rho E(u)du] > 0, \\
I_e(t) &= e^{-(\gamma_3+d)t}[I_e(0) + \int_0^t \alpha(1-\rho)E(u)du] > 0, \\
Q(t) &= e^{-(\gamma_2+d+m)t}[Q(0) + \int_0^t pI(u)du] > 0, \\
R(t) &= e^{-(\eta_1+\eta_2+d)t}[R(0) + \int_0^t (\gamma_1 I(u) + \gamma_2 Q(u) + \gamma_3 I_e(u))du] > 0, \\
W(t) &= e^{-\delta t}[W(0) + \int_0^t (\lambda_1 I(u) + \lambda_2 I_e(u))du] > 0.
\end{aligned}$$

This means that $\varphi(t) \notin \partial X_0$ for $t > 0$, which contradicts the assumption that $\varphi(t) \in M_\partial$. Hence, we obtain that $M_\partial \subseteq M'_\partial$. Since $M_\partial = M'_\partial$, we obtain that M_∂ only has the disease-free equilibrium $E_0(S^0, V^0, 0, 0, 0, 0, 0, 0)$ and E_0 is compact and isolate invariant for $\varphi(0) \in M_\partial$.

Next, we only need to prove that $W^s(E_0) \cap X_0 = \emptyset$, where $W^s(E_0)$ denotes the stable manifold of E_0. That is, there exists a positive constant ε such that for any solution $\Phi_t(\varphi(0))$ of system (2.1) with the initial condition $\varphi(0) \in X_0$, one has

$$D(\Phi_t(\varphi(0)), E_0)^\infty \geq \varepsilon,$$

where D is a distance function in X_0. Suppose not, then $D(\Phi_t(\varphi(0)), E_0)^\infty < \bar{\varepsilon}$, for $\forall \bar{\varepsilon} > 0$. Hence, there must exists $T > 0$ such that $\frac{\Lambda}{k+d} - \bar{\varepsilon} \leq S(t) \leq \frac{\Lambda}{k+d} + \bar{\varepsilon}$, $\frac{k\Lambda}{d(k+d)} - \bar{\varepsilon} \leq V(t) \leq \frac{k\Lambda}{d(k+d)} + \bar{\varepsilon}$, $0 \leq E(t) \leq \bar{\varepsilon}$, $0 \leq I(t) \leq \bar{\varepsilon}$, $0 \leq Q(t) \leq \bar{\varepsilon}$ and $0 \leq W(t) \leq \bar{\varepsilon}$, for $t > T$. For $t > T$, we have

$$\begin{cases}
\dfrac{dE}{dt} \geq L_1(\bar{\varepsilon})I + L_2(\bar{\varepsilon})I_e + L_3(\bar{\varepsilon})W - (\alpha + d)E, \\
\dfrac{dI}{dt} = \alpha\rho E - (p + \gamma_1 + d + m)I, \\
\dfrac{dI_e}{dt} = \alpha(1-\rho)E - (\gamma_3 + d)I_e, \\
\dfrac{dW}{dt} = \lambda_1 I + \lambda_2 I_e - \delta W,
\end{cases} \tag{3.25}$$

where

$$L_1(\bar{\varepsilon}) = \beta_1(\frac{\Lambda}{k+d} - \bar{\varepsilon}) + \bar{\beta}_1(\frac{k\Lambda}{d(k+d)} - \bar{\varepsilon}),$$
$$L_2(\bar{\varepsilon}) = \beta_2(\frac{\Lambda}{k+d} - \bar{\varepsilon}) + \bar{\beta}_2(\frac{k\Lambda}{d(k+d)} - \bar{\varepsilon}),$$
$$L_3(\bar{\varepsilon}) = \sigma(\frac{\Lambda}{k+d} - \bar{\varepsilon}) + \bar{\sigma}(\frac{k\Lambda}{d(k+d)} - \bar{\varepsilon}).$$

Consider an auxiliary system as follows

$$\frac{du}{dt} = \bar{A}(\bar{\varepsilon})u, \tag{3.26}$$

where $u = (u_1, u_2, u_3, u_4)^T$ and

$$\bar{A}(\bar{\varepsilon}) = \begin{pmatrix} -(\alpha+d) & L_1(\bar{\varepsilon}) & L_2(\bar{\varepsilon}) & L_3(\bar{\varepsilon}) \\ \alpha\rho & -(p+\gamma_1+d+m) & 0 & 0 \\ \alpha(1-\rho) & 0 & -(\gamma_3+d) & 0 \\ 0 & \lambda_1 & \lambda_2 & -\delta \end{pmatrix}. \tag{3.27}$$

Recall that stability modulus of matrix $\bar{A}(\bar{\varepsilon})$, denoted by $S(\bar{A}(\bar{\varepsilon}))$, is defined by

$$S(\bar{A}(\bar{\varepsilon})) = \max\{\text{Re } \lambda\colon \lambda \text{ is an eigenvalue of } \bar{A}(\bar{\varepsilon})\}.$$

Note that $\bar{A}(\bar{\varepsilon})$ is irreducible and has non-negative off-diagonal elements, then $S(\bar{A}(\bar{\varepsilon}))$ is a simple eigenvalue of $\bar{A}(\bar{\varepsilon})$ with a positive eigenvector (see Theorem A. 5 in [43]). By Lemma 2.1 in [44] and the proof of Theorem 2 in [41], the following equivalent inequations are hold:

$$R_0 < 1 \Longleftrightarrow S(\bar{A}(0)) < 0, \text{ and } R_0 > 1 \Longleftrightarrow S(\bar{A}(0)) > 0. \tag{3.28}$$

Since $S(\bar{A}(\bar{\varepsilon}))$ is continous in $\bar{\varepsilon}$, choose $\bar{\varepsilon} > 0$ small enough such that $S(\bar{A}(\bar{\varepsilon})) > 0$ as $R_0 > 1$. Hence, let $u(t) = (u_1(t), u_2(t), u_3(t), u_4(t))^T$ be a positive solution of the auxiliary system (3.26), which is strictly increasing with $u_i(t) \to +\infty$ as $t \to +\infty$, $i = 1, \ldots, 4$. By the comparison principle, one has

$$\lim_{t\to+\infty} E(t) = +\infty, \lim_{t\to+\infty} I(t) = +\infty, \lim_{t\to+\infty} I_e(t) = +\infty, \lim_{t\to+\infty} W(t) = +\infty. \tag{3.29}$$

By system (2.1), since

$$\lim_{t\to+\infty} I(t) = +\infty, \lim_{t\to+\infty} I_e(t) = +\infty,$$

it is also gained that

$$\lim_{t\to+\infty} Q(t) = +\infty, \lim_{t\to+\infty} R(t) = +\infty.$$

This contracts with our assumption. Hence, E_0 is an isolated invariant set in X and $W^s(E_0) \cap X_0 = \emptyset$.

Therefore, the system (2.1) is uniformly persistent if $R_0 > 1$. This completes the proof. □

Remark 2. As far as the authors' knowledge, all the existing results of autonomous epidemiological models for HFMD such as [28, 29, 31, 34, 35, 40] have obtained the similar result that the basic reproduction number R_0 is the only criterion to determine whether the disease is eliminated, i.e., the model only has a disease-free equilibrium if $R_0 < 1$ and it is uniformly persistent if $R_0 > 1$. Because we consider vaccination and the vaccinated individuals can also be infected by HFMD viruses except EV71 in modeling, different from the existing results, the disease is extinct as $\hat{R}_0 < 1$ (see Theorem 3.4). In addition, our model may have positive equilibriums even if the basic reproduction number R_0 is less than 1 (see the analyses in Section 5).

In particular, if we ignore the influence of vaccination, i.e., let $k = 0$ for system (2.1) and define the model as $SEII_eQRW$, then the reproduction number for $SEII_eQRW$ is defined as

$$\check{R}_0 = \Big\{ \frac{\rho\alpha\beta_1}{(\alpha+d)(p+\gamma_1+d+m)} + \frac{(1-\rho)\alpha\beta_2}{(\alpha+d)(\gamma_3+d)} + \Big(\frac{\alpha\rho\lambda_1}{(\alpha+d)(p+\gamma_1+d+m)\delta} + \frac{\alpha(1-\rho)\lambda_2}{(\alpha+d)(\gamma_3+d)\delta} \Big)\sigma \Big\} \frac{\Lambda}{d}.$$

By using the similar analysis as that in the proof of Theorem 3.3 and Theorem 3.4, one can easily derive the following corollary. Its proof is omitted.

Corollary 1. *If $\check{R}_0 < 1$, then system $SEII_eQRW$ has an unique disease-free equilibrium $\check{E}_0(S^0, E^0, I^0, I_e^0, Q^0, R^0, W^0) = (\frac{\Lambda}{d}, 0, 0, 0, 0, 0, 0)$ and $\check{E}_0$ is globally asymptotically stable; If $\check{R}_0 > 1$, then system $SEII_eQRW$ is uniformly persistent.*

From Corollary 1, it is clear that $\check{R}_0$ is the only threshold to decide whether the disease is extinct or not.

4. Numerical analysis

In this section, by using system (2.1), we simulate the reported data of HFMD in mainland China. From the website of CCDC [3], and NHFPC [18], we have obtained the monthly numbers of newly reported HFMD cases in mainland China from January 2015 to December 2017. We only consider the population of young children under six years old, a high risk group for HFMD. Note that EV71 virus has been vaccinated in mainland China starting in 2016, then we assume that the vaccinated rate k of system (2.1) is zero before 2016.

4.1. Data fitting

First, based on BP neural network, we design an algorithm to estimate unknown parameters of system (2.1) (see Appendix A) to. Then, we estimate parameters of system (2.1) by minimizing the following error function

$$ER = \sum_{i=1}^{12} (I_i - \hat{I}_i)^2 / N, \tag{4.1}$$

where $\hat{I}_i$ is the reported data of HFMD in the i month. I_i is numerically computed solutions of $I(t)$ of system (2.1) in the i month. N is the annual total population of less than 6 years old.

Table 2. The values of parameters and initial conditions for system (2.1) from 2015 to 2017 (unit: month^{-1})

Para.	2015	2016	2017	References
Λ	1382638	1488333	1518641	[45]
m	6.46×10^{-5}	3.42×10^{-4}	1.27×10^{-4}	[3, 18]
β_1	1.08×10^{-7}	1.11×10^{-7}	1.08×10^{-7}	Fitting
β_2	2.44×10^{-8}	2.50×10^{-8}	2.38×10^{-7}	Fitting
σ	7.61×10^{-11}	7.51×10^{-11}	7.6×10^{-11}	Fitting
$\bar{\beta}_1$	0	6.76×10^{-8}	6.58×10^{-8}	Fitting
$\bar{\beta}_2$	0	1.38×10^{-8}	1.38×10^{-8}	Fitting
$\bar{\sigma}$	0	5.65×10^{-11}	4.47×10^{-11}	Fitting
d	1.42×10^{-2}	1.28×10^{-2}	1.31×10^{-2}	[45]
k	0	1.21×10^{-3}	1.31×10^{-3}	Fitting
η_1	0.035	0.035	0.035	[31]
η_2	0	1.5×10^{-6}	1.5×10^{-6}	Assumption
$1/\alpha$	4/30	4/30	4/30	[28]
ρ	0.2294	0.2299	0.2316	Fitting
γ_1	3.5293	3.5293	3.5293	[28]
γ_2	3.5293	3.5293	3.5293	[28]
γ_3	3.5293	3.5293	3.5293	Assumption
p	0.0025	0.0025	0.0025	[30]
λ_1	93.8	93.8	93.8	[31]
λ_2	78.9	78.9	78.9	[31]
δ	2.7	2.7	2.7	[31]
$S(0)$	95020000	96288000	95820000	[45]
$V(0)$	0	0	5×10^5	Assumption
$E(0)$	300000	300000	300000	Assumption
$I(0)$	57763	79499	77412	[3, 18]
$I_e(0)$	150000	150000	150000	Assumption
$Q(0)$	0	0	0	Assumption
$R(0)$	28000	28000	28000	Assumption
$W(0)$	0	0	0	Assumption

Table 3. The fitting error ER (4.1) between the reported HFMD cases in mainland China and the simulation of $I(t)$ of system (2.1).

Year	2015	2016	2017
ER	3.47×10^{-6}	8.54×10^{-6}	3.86×10^{-6}

All the estimated parameters are shown in Table 2, and the error ER for every year is computed and included in Table 3. It is obvious that $ER < 0.0001$ in every year. Therefore, our model fits well with the reported data of HFMD for each year from 2015 to 2017 in mainland China. Taking the year of 2017 as an example, the numerical simulation of the number of symptomatic infectious individuals $I(t)$

of HFMD by system (2.1) is shown in Figure 3.

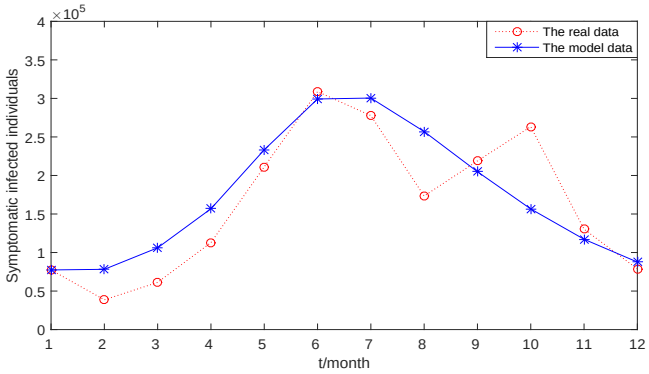

Figure 3. The comparison between the reported HFMD cases in mainland China and the simulation of $I(t)$ of system (2.1) in 2017. The values of parameters and the initial values are given in Table 2.

4.2. Sensitivity analysis

We all know that the basic reproduction number R_0 is an important quantity in characterizing the spread of disease.

Table 4. The values of the basic reproduction number from 2015 to 2017.

Year	2015	2016	2017
R_1	0.6651	0.6535	0.6377
R_2	0.4011	0.4418	0.4066
R_3	0.0515	0.0546	0.0532
R_0	1.1177	1.1499	1.0975

Based on the basis of our parameter values, the basic reproduction number R_0 and basic components of R_0 include R_1, R_2, R_3 are calculated in every year in Table 4. Note that the basic reproduction $R_0 = R_1 + R_2 + R_3$ for each year is greater than 1, where R_1, R_2, and R_3 with respect to symptomatic infected, asymptomatic infected individual, and free-living viruses in the environment, respectively. Moreover, in Table 4, the values of R_1 and R_2 are far greater than R_3, which means that the new patient has a high probability of being infected by symptomatic infectious individuals and asymptomatic infectious individuals, rather than the contaminated environment caused by infectious individuals.

Next, by using Latin hypercube sampling (LHS) and partial rank correlation coefficients (PRCCS) [46] (Marino et al., 2008), we investigate the effects of parameters on R_0. It notes that PRCCS, showing which parameters have the largest influence on model outcomes, is calculated using the rank transformed LHS matrix and output matrix [46]. Take 2000 simulations per round, choose a uniform distribution for all the parameters with ranges listed in Table 5, and test for significant PRCCs for all parameters of system (2.1).

Figure 4 shows that the PRCC values illustrate the dependence of R_0 on each input parameter. Assume that absolute values of PRCC$>$ 0.4 is highly negatively correlated between input parameters and R_0, then it is easy to know that $\beta_1, \beta_2, \sigma, \bar{\beta}_1, \bar{\beta}_2, \lambda_2$ are highly positively correlated to R_0, while

Table 5. PRCC values for R_0.

Parameter	Distribution	PRCC	p-Value
Λ	$U(1.38\times10^{6}, 1.53\times10^{6})$	0.2692	2.49×10^{-5}
β_1	$U(1.05\times10^{-7}, 1.25\times10^{-7})$	0.9705	0
β_2	$U(2.2\times10^{-8}, 2.6\times10^{-8})$	0.8901	0
σ	$U(7.0\times10^{-11}, 8.0\times10^{-11})$	0.4059	0
$\bar{\beta}_1$	$U(6.5\times10^{-8}, 7.0\times10^{-8})$	0.5397	0
$\bar{\beta}_2$	$U(1.1\times10^{-8}, 1.5\times10^{-8})$	0.4250	0
$\bar{\sigma}$	$U(4.0\times10^{-11}, 6.0\times10^{-11})$	0.0729	1.04×10^{-11}
k	$U(1.1\times10^{-3}, 1.5\times10^{-3})$	-0.7439	0
d	$U(1.2\times10^{-2}, 1.5\times10^{-2})$	-0.1280	0.0013
α	U(7.3, 7.7)	0.00173	0.0943
ρ	U(0.22, 0.25)	0.1351	0
γ_1	U(3.4, 3.6)	-0.8908	0
γ_3	U(3.4, 3.6)	-0.8101	0
λ_1	U(85, 95)	0.1833	3.44×10^{-15}
λ_2	U(75, 85)	0.6495	0
δ	U(2.5, 3.0)	-0.7123	0
m	$U(5.0\times10^{-5}, 4.0\times10^{-4})$	-0.00215	0.0029
p	$U(2.0\times10^{-3}, 3.0\times10^{-3})$	-0.5388	0

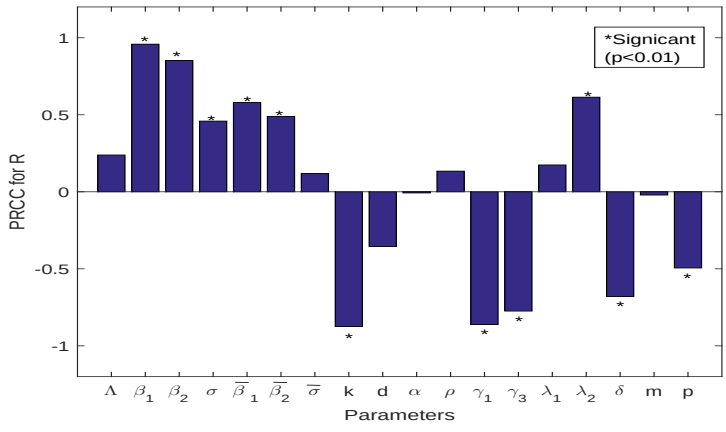

Figure 4. The values of correlation coefficient for outcome R_0.

$k, \gamma_1, \gamma_3, \delta, p$ are highly negatively correlated to R_0. That is, reducing positively correlated parameters and increasing negatively correlated parameters can reduce value of R_0, in which lower value of R_0 means lower spread of the epidemics.

4.3. Prevention and control strategies

According to sensitivity analysis of R_0 in Subsection 4.2, we have known the key factors affecting the spread of HFMD. Then, some detailed numerical experiments provide effective measures for the prevention and control of the spread of FHMD in mainland China. Moreover, we pay more attention to that the varieties of vaccinated individuals, quarantined individuals, and environmental health impact HFMD epidemic in mainland China, which can be shown by adjusting the related parameters k, p, δ for system (2.1). Taking the year of 2017 as an example, the prevention and control strategies are proposed as follows:

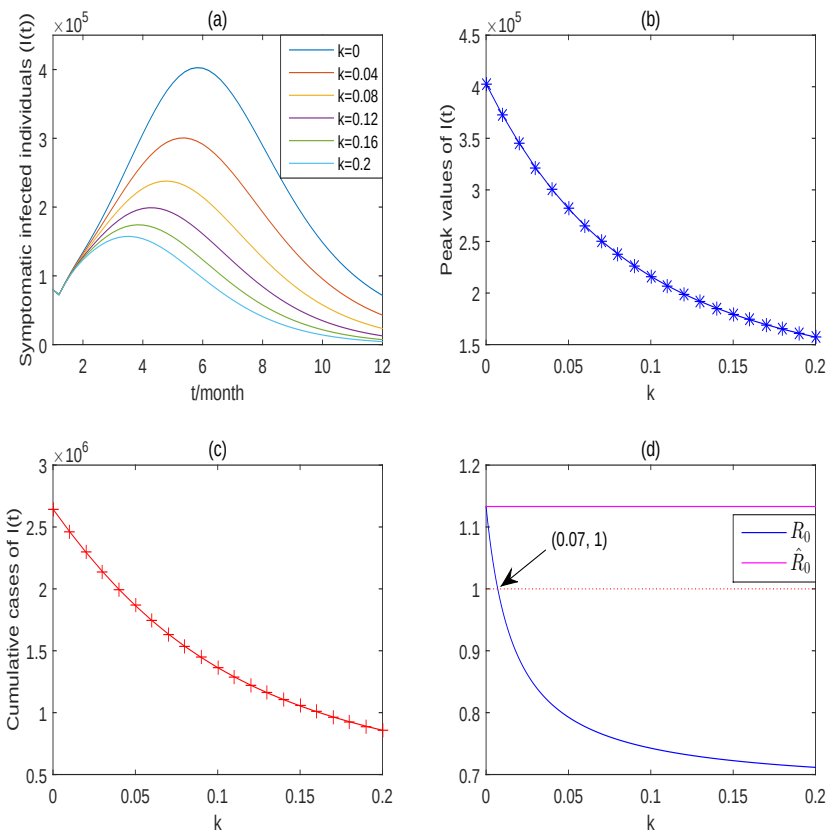

Figure 5. Simulations of system (2.1) for numbers of the symptomatic infected individuals $I(t)$ with respect to parameter k. (a) Epidemic curves of $I(t)$; (b) Peak values of $I(t)$; (c) Annual cumulative cases of $I(t)$; (d) Values of R_0 and $\hat{R}_0$. Other parameter values are given in Table 2.

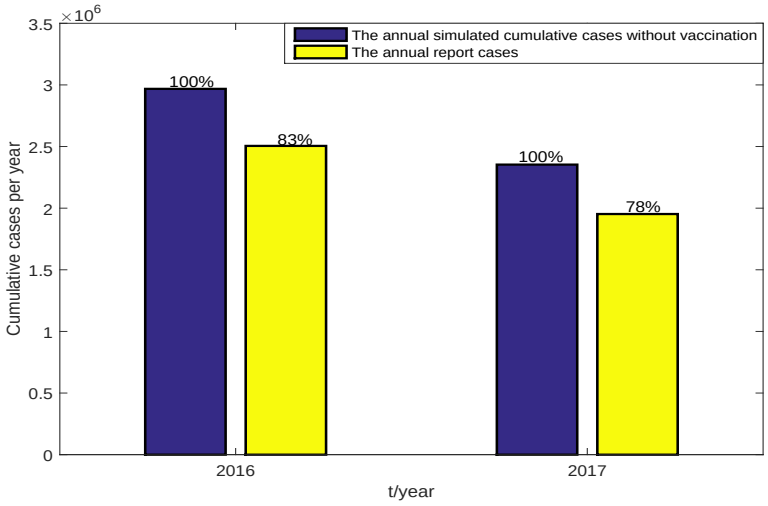

Figure 6. The comparison between the annual simulated cumulative cases by system (2.1) without vaccination (assume $k = 0$) and annual reported cumulative cases for HFMD in mainland China from 2016 to 2017. The ratios of the reported data to the simulation data are shown in histogram. The values of other parameters and the initial values are given in Table 2.

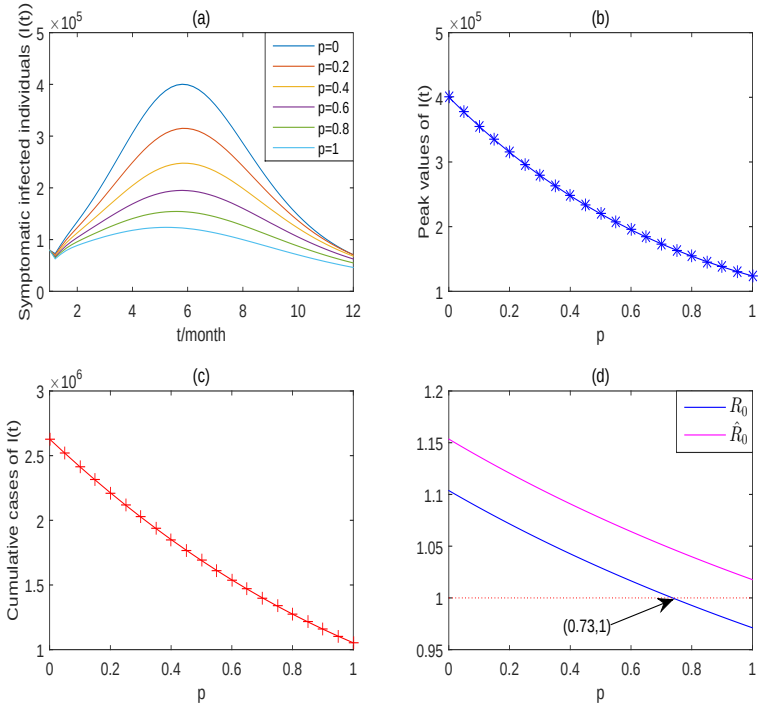

Figure 7. Simulations of system (2.1) for numbers of the symptomatic infected individuals $I(t)$ with respect to parameter p. (a) Epidemic curves of $I(t)$; (b) Peak values of $I(t)$; (c) Annual cumulative cases of $I(t)$; (d) Values of R_0 and $\hat{R}_0$. Other parameter values are given in Table 2.

Strategy 1: Increasing the vaccinated rate k for the susceptible individuals $S(t)$ can reduce the spread of HFMD. Though the vaccinated individuals $V(t)$ can also be infected, but they have a lower infected probability than the unvaccinated individuals $S(t)$. In Table 2, all transmission rates of $V(t)$ of system (2.1) such as $\bar{\beta}_1, \bar{\beta}_2$ and $\bar{\sigma}$ are smaller than the transmission rates of $S(t)$. Figure 5 (a) shows that the simulation of $I(t)$ of system (2.1) decreases with increasing the vaccinated rate k, while the solution curve of symptomatic infected individuals $I(t)$ of system (2.1) is at the top in the figure as $k = 0$. Moreover, Figure 5 (b) and Figure 5 (c) show that the peak values and annual cumulative cases of symptomatic infected individuals $I(t)$ decreases with the increase of k. Except for parameter k, Assuming that all the parameter of system (2.1) are shown in Table 1, and comparing Figure 5 (d) with Figure 5 (a), Figure 5 (b) and Figure 5 (c), we obtain the following results: (i) The size of R_0 determines the degree of the disease outbreaks, which are the same as the analyses in Subsection 4.2; (ii) If the vaccinated rate $k < 0.07$, i.e., $R_0 < 1$, then the disease persists (see Theorem 3.3); (iii) If the vaccinated rate $k > 0.07$, which means that $R_0 < 1$ and $\hat{R}_0 > 1$, then we can not be sure whether the disease disappears or persists (see Theorem 3.3 and Theorem 3.4, and the reasons are analyzed in detail in Section 5). Furthermore, In order to investigate the effects of current EV71 vaccination strategy for HFMD in mainland China, we compare the annual simulated cumulative cases by system (2.1) without vaccination with the report cases. In Figure 6, the annual reported cumulative cases are lower than the annual simulation cumulative cases, and we also obtain that the current vaccine measures have reduced the total number of patients in 2016 and 2017 by 17% and 22%, respectively.

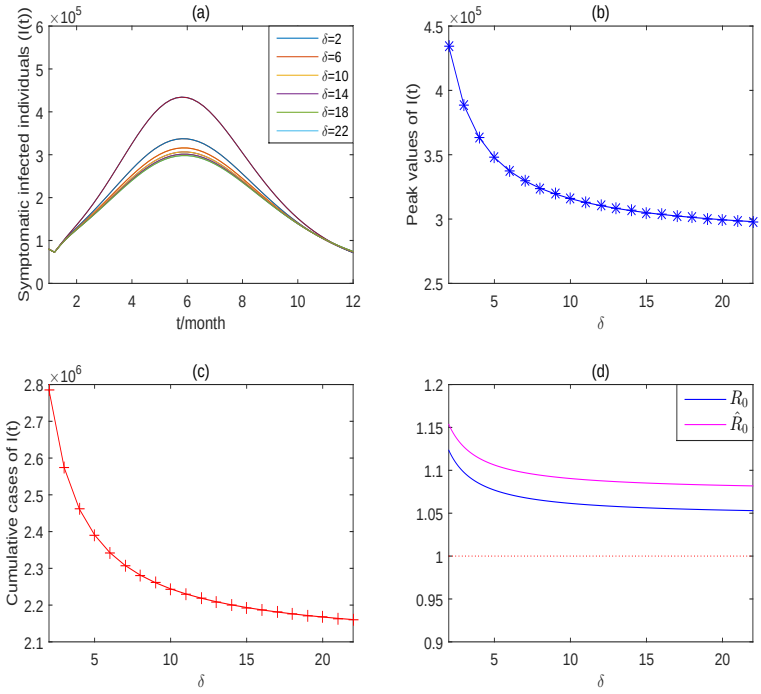

Figure 8. Simulations of system (2.1) for numbers of the symptomatic infected individuals $I(t)$ with respect to parameter δ. (a) Epidemic curves of $I(t)$; (b) Peak values of $I(t)$; (c) Annual cumulative cases of $I(t)$; (d) Values of R_0 and $\hat{R}_0$. Other parameter values are given in Table 2.

Strategy 2: Increasing the quarantined rate p for the symptomatic infectious individuals $I(t)$ can reduce the spread of HFMD. From system (2.1), the quarantined individuals $Q(t)$ can not spread diseases and the symptomatic infectious individuals $I(t)$ are highly infectious, then transforming the symptomatic infectious into the quarantined is an efficient control strategy. From Figure 7 (d), we obtain that the disease persists if the quarantined rate $p < 0.73$, while the long-term behaviors of the disease may not be ensure if $p > 0.73$. The other analyses for Figure 7 are the same as strategy 1.

Strategy 3: Increasing the clearance rate δ of the pathogens caused by the infectious individuals containing $I(t)$ and $I_e(t)$ can reduce the spread of HFMD (see Figure 8). For instance, we can improve health-care education such as washing hands after using the toilet and before meals, and making air fresh indoors and so on. It should popularize health knowledge and advocate good personal hygiene habits in kindergardens, schools, hospitals and other places. Kindergardens should clean and disinfect toys and appliances every day. Moreover, hospitals should strengthen infection control practices to avoid nosocomial cross infection. In addition, from Figure 8 (d), the disease persists.

In short, if we use the above prevention and control measures, the HFMD would be effectively controlled and the number of infections would decrease rapidly in short time. Those measures can effectively prevent and control the large-scale diffusion of HFMD in mainland China.

5. Discussion and conclusion

In this paper, we have proposed an eight-compartment dynamic model for HFMD in mainland China. The proposed model extends the existing models by considering vaccination, contaminated environment and quarantine simultaneously, where the vaccinated individuals with EV71 vaccine can also be infected by other FHMD viruses and the transmission rates with respect to the vaccinated individuals may be different from the unvaccinated individuals. Hence, unlike the previous results, we take the vaccinated individuals as an independent compartment in modeling. The main purpose of this study is to examine the effect of vaccination, contaminated environment and quarantine on the spread of HFMD in mainland China.

By investigating the dynamic behaviors of our model, we have identified two critical parameters as the basic reproduction number R_0 and the threshold parameter $\hat{R}_0$ ($R_0 \leq \hat{R}_0$). Then, the dynamic behaviors of system (2.1) could be divided into three cases (see Section 3):

(i) If $R_0 \leq \hat{R}_0 < 1$, then system (2.1) has only one disease-free equilibrium E_0 and E_0 is globally asymptotically stable, which means that the disease is extinct (see Theorem 3.3);

(ii) If $1 < R_0 \leq \hat{R}_0$, then system (2.1) is uniformly persistent (see Theorem 3.4);

(iii) If $R_0 < 1 < \hat{R}_0$, then dynamic behaviors of system (2.1) are difficult to determine.

Unlike the previous results of epidemiological models for HFMD [28, 29, 31, 34, 35, 40], in which the disease-free equilibrium is globally asymptotically stable if the basic reproduction number $R_0 < 1$, in case (iii) that E_0 of system (2.1) may not be globally asymptotically stable and system (2.1) may have positive equilibriums. For example, if take $\Lambda = 1.3 \times 10^4, \beta_1 = 2.29 \times 10^{-7}, \beta_2 = 1.5 \times 10^{-7}, \sigma = 1 \times 10^{-7}, \bar{\beta}_1 = 0.1 \times 10^{-7}, \bar{\beta}_2 = 1 \times 10^{-7}, \bar{\sigma} = 0.7 \times 10^{-7}, \alpha = 0.4, \rho = 0.5, \eta_1 = 2.29, \eta_2 = 1.5, \gamma_1 = 0.9, \gamma_2 = 2, \gamma_3 = 0.9, \lambda_1 = 0.04, \lambda_2 = 0.04, \delta = 0.4, d = 1 \times 10^{-3}, p = 0.1, k = 0.1, m = 1 \times 10^{-4}$ for system (2.1) , then we obtain a disease-free equilibrium

$$E_0(S^0, V^0, E^0, I^0, I_e^0, Q^0, R^0, W^0) = (1.2871 \times 10^5, 1.2871 \times 10^7, 0, 0, 0, 0, 0, 0)$$

and a positive equilibrium (see Figure 9)

$$E_*(S^*, V^*, E^*, I^*, I_e^*, Q^*, R^*, W^*) = (3.7283 \times 10^6, 3.3361 \times 10^6, 4.0799 \times 10^6, 8.1508 \times 10^5, 9.0564 \times 10^5, 4.0732 \times 10^4, 1.6302 \times 10^4, 1.7207 \times 10^5).$$

Based on the above parameter values, we calculate $R_0 = 0.8981$ and $\hat{R}_0 = 2.6993$. Then, in this case, when $R_0 < 1 < \hat{R}_0$, it is obvious that system (2.1) has a disease-free equilibrium and a positive equilibrium, and none of them is globally asymptotically stable. The reason our model has dynamic behaviors different from those seen in the existing research is that our model considers vaccination, and the vaccinated individuals can also be infected by HFMD viruses except EV71; thus, the reproduction number R0 can not be the only threshold to judge whether the disease is extinct or not.

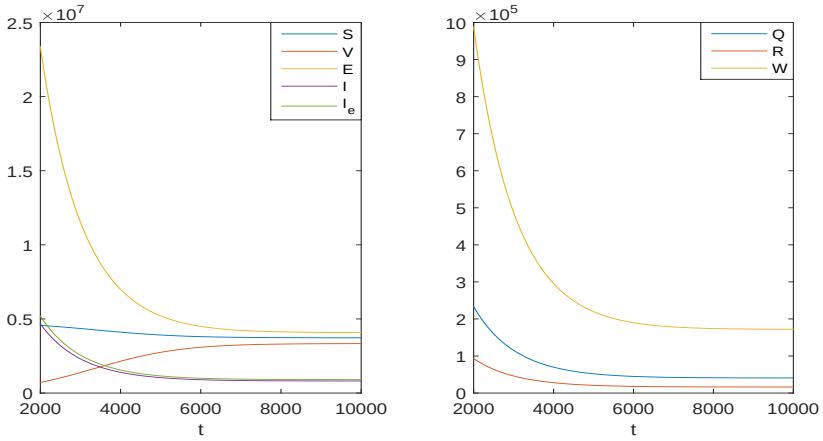

Figure 9. Simulations of model (2.1).

The proposed model has been used to individually fit the annual reported cases of HFMD in mainland China from 2015 to 2017. Moreover, the basic reproduction number R_0 of each year is greater than 1 (see Table 4), which means system (1) is uniformly persistent. Using Latin hypercube sampling (LHS) and partial rank correlation coefficients (PRCCS) for sensitive analysis of R_0, we find the key factors affecting transmission of HFMD, where the highly positively correlated parameters are $\beta_1, \beta_2, \sigma, \bar{\beta}_1, \bar{\beta}_2, \lambda_2$ and the highly negatively correlated parameters are $k, \gamma_1, \gamma_3, \delta, p$ (see Subsection 4.2). We analyse effect of the varieties of the rates k, δ and p, with respect to vaccinated individuals, quarantined individuals and environmental health respectively, on the spread of HFMD in mainland China. As a result, we deduce that increasing the rates k, δ, p can reduce the number of infectious individuals in detail in Subsection 4.3. Moreover, it also easily verifies that for any $k > 0$ or $\delta > 0$ or $p > 0$, the threshold parameter $\hat{R}_0 > 1$. This means that our control strategies can reduce the spread of FHMD in mainland China, but the disease may not go extinct in mainland China. To eliminate the disease, it is necessary to reduce the rates $\beta_1, \beta_2, \sigma, \bar{\beta}_1, \bar{\beta}_2$ and γ_1, γ_3, but this is usually very difficult, in that the average contact rate of children may be hard to control and because in mainland China, medical conditions are difficult to improve over a short period.

It should be mentioned that we fitted our proposed model to the reported data and estimated some unknown parameters in each year, so that it is not necessary to consider seasonal infection variations of this disease. Note that HFMD is a typical seasonal disease, which is usually affected by

temperature and humidity [19, 30, 33, 36]. In the future, we will model periodic infection of the disease together with vaccination, contaminated environment, and quarantine. The authors thank the anonymous referees, whose careful reading, insights, valuable comments, and suggestions significantly enabled us to improve the quality of the paper.

Acknowledgments

H. Zhao is supported by the National Natural Science Foundation of China (No 11571170). D. Wu is supported by the Natural Science Foundation of Anhui Province of China (No 1608085MA14), and the Programs of Educational Commission of Anhui Province of China (No KJ2015A152). The authors thank anonymous reviewers for their valuable comments. Their comments have enhanced the clarity and the quality.

Conflict of interest

All authors declare no conflicts of interest in this paper.

References

1. F. C. Tseng, H. C. Huang, C. Y. Chi, T. L. Lin, C. C. Liu, J. W. Jian, L. C. Hsu, H. S. Wu, J. Y. Yang and Y. W. Chang, Epidemiological survey of enterovirus infections occurring in Taiwan between 2000 and 2005: analysis of sentinel physician surveillance data, *J. Med. Virol.*, **79** (2007), 1850–1860.
2. Q. Zhu, Y. Hao, J. Ma, S. Yu and Y. Wang, Surveillance of hand, foot, and mouth disease in mainland China (2008-2009), *Biomed. Environ. Sci.*, **24** (2011), 349–356.
3. Chinese Center for Disease Control and Prevention (CCDC), *National Public Health Statistical Data*. 2018 Available from: http://www.chinacdc.cn/tjsj/fdcrbbg/index.html.
4. N. J. Schmidt, E. H. Lennette and H. H. Ho, An apparently new enterovirus isolated from patients with disease of the central nervous system, *J. Infect. Dis.*, **129** (1974), 304–309.
5. G. L. Repass, W. C. Palmer and F. F. Stancampiano, Hand, foot and mouth disease: identifying and managing an acute viral syndrome, *Clev. Clin. J. Med.*, **81** (2014), 537–543.
6. M. Cabrerizo, D. Tarragó, C. Muñoz-Almagro, A. E. Del, M. Domínguez-Gil, J. M. Eiros, I. López-Miragaya, C. Pérez, J. Reina and A. Otero, Molecular epidemiology of enterovirus 71, coxsackievirus A16 and A6 associated with hand, foot and mouth disease in Spain, *Clin. Microbiol. Infec.*, **20** (2014), O150–O156.
7. S. Ljubin-Sternak, V. Slavic-Vrzic, T. Vilibić-Čavlek and I. Gjenero-Margan, Outbreak of hand, foot and mouth disease caused by coxsackie A16 virus in a childcare center in croatia, *European Communicable Disease Bulletin*, **21** (2011), 9–11.
8. N. Sarma, A. Sarkar, A. Mukherjee, A. Ghosh, S. Dhar and R. Malakar, Epidemic of hand, foot and mouth disease in west bengal, india in august, 2007: a multicentric study, *Indian J. Dermatol.*, **54** (2009), 26–30.

9. O. M. How, W. S. Chang, M. Anand, P. Yuwana, P. David, C. Daniella, D. S. Sylvia, C. C. Hee, T. P. Hooi and C. M. Jane, Identification and validation of clinical predictors for the risk of neurological involvement in children with hand, foot, and mouth disease in Sarawak, *Bmc Infect. Dis.*, **9** (2009), 3–3.
10. T. Fujimoto, M. Chikahira, S. Yoshida, H. Ebira, A. Hasegawa, A. Totsuka and O. Nishio, Outbreak of central nervous system disease associated with hand, foot, and mouth disease in Japan during the summer of 2000: detection and molecular epidemiology of enterovirus 71, *Microbiol. Immunol.*, **46** (2002), 621–627.
11. J. Wang, Z. Cao, D. D. Zeng, Q. Wang, X. Wang and H. Qian, Epidemiological analysis, detection, and comparison of space-time patterns of Beijing hand-foot-mouth disease (2008-2012), *PLoS One*, **9** (2014). Article ID: e92745.
12. W. S. Ryu, B. Kang, J. Hong, S. Hwang, J. Kim and D. S. Cheon, Clinical and etiological characteristics of enterovirus 71-related diseases during a recent 2-year period in Korea, *J. Clin. Microbiol.*, **48** (2010), 2490–2494.
13. J. Cheng, J. Wu, Z. Xu, R. Zhu, X. Wang, K. Li, L. Wen, H. Yang and H. Su, Associations between extreme precipitation and childhood hand, foot and mouth disease in urban and rural areas in Hefei, China, *Sci. Total Environ.*, **497** (2014), 484–490.
14. H. X. Nguyen, C. Chu, H. L. T. Nguyen, H. T. Nguyen, C. M. Do, S. Rutherford and D. Phung, Temporal and spatial analysis of hand, foot, and mouth disease in relation to climate factors: A study in the Mekong Delta region, Vietnam, *Sci. Total Environ.*, **581** (2017), 766–772.
15. F. Gou, X. Liu, X. Ren, D. Liu, H. Liu, K. Wei, X. Yang, Y. Cheng, Y. Zheng and X. Jiang, Socio-ecological factors and hand, foot and mouth disease in dry climate regions: a Bayesian spatial approach in Gansu, China, *Int. J. Biometeorol.*, **61** (2017), 137–147.
16. W. Jing, T. Hu, D. Sun, S. Ding, M. J. Carr, W. Xing, S. Li, X. Wang and W. Shi, Epidemiological characteristics of hand, foot, and mouth disease in Shandong, China, 2009-2016, *Sci. Rep.*, **7** (2017). Article ID: 8900.
17. Y. Weng, W. Chen, W. He, M. Huang, Y. Zhu and Y. Yan, Serotyping and genetic characterization of hand, foot, and mouth disease (HFMD)-associated enteroviruses of no-ev71 and non-cva16 circulating in fujian, china, 2011-2015, *Med. Sci. Monitor*, **23** (2017), 2508–2518.
18. National Health and Family Planning Commission of the Peoples Republic of China (NHFPC), *China Health Statistical Yearbook*. 2018 Available from: http://www.moh.gov.cn/zwgk/yqbb3/ejlist.shtml.
19. Z. Chang, F. Liu, L. Bin, Z. Wang and L. Zeng, Analysis on surveillance data of hand, foot and mouth disease in China, January - May 2017, *Disease Surveillance*, **32** (2017), 447–452.
20. Y. Cao, Z. Hong, L. Jin, O. U. Jian-Ming and R. Hong, Surveillance of hand, foot and mouth disease in China, 2011-2012, *Disease Surveillance*, **28** (2013), 975–980.
21. J. Sun, Z. Chang, L. Wang and L. Wang, Analysis on the epidemic situation of hand, foot and mouth disease in China in January - March, 2013, *Practical Prev. Med.*, **21** (2014), 183–186.
22. J. T. Wu, M. Jit, Y. Zheng, K. Leung and W. Xing, Routine pediatric enterovirus 71 vaccination in China: a cost-effectiveness analysis, *Plos Med.*, **13** (2016). Article ID: e1002013.

23. S. Takahashi, Q. Liao, T. P. Van Boeckel, W. Xing, J. Sun, V. Y. Hsiao, C. J. Metcalf, Z. Chang, F. Liu and J. Zhang, Hand, foot, and mouth disease in China: modeling epidemic dynamics of enterovirus serotypes and implications for vaccination, *Plos Med.*, **13** (2016). Article ID: e1001958.
24. N. Ziyadi, A male-female mathematical model of human papillomavirus (HPV) in African American population, *Math. Biosci. Eng.*, **14** (2017), 339–358.
25. S. Liu, Y. Li, Y. Bi, and Q. Huang, Mixed vaccination strategy for the control of tuberculosis: A case study in China, *Math. Biosci. Eng.*, **14** (2017), 695–708.
26. M. L. Manyombe, J. Mbang, J. Lubuma and B. Tsanou, Global dynamics of a vaccination model for infectious diseases with asymptomatic carriers, *Math. Biosci.*, **13** (2016), 813–840.
27. Y. C. Wang and F. C. Sung, Modeling the infections for Enteroviruses in Taiwan, *Taipei: Institute of Environmental Health (2006)*. Article ID: 228559790.
28. F. C. S. Tiing and J. Labadin, A simple deterministic model for the spread of hand, foot and mouth disease (HFMD) in Sarawak, *2008 Second Asia International Conference on Modelling & Simulation*, (2008), 947–952.
29. N. Roy, Mathematical modeling of hand-foot-mouth disease: quarantine as a control measure, *Int. J. Adv. Sci. Eng. Technol. Res.*, **1** (2012), 1–11.
30. Y. Ma, M. Liu, Q. Hou and J. Zhao, Modelling seasonal HFMD with the recessive infection in Shandong, China, *Math. Biosci. Eng.*, **10** (2013), 1159–1171.
31. J. Wang, Y. Xiao and R. A. Cheke, Modelling the effects of contaminated environments on HFMD infections in mainland China, *Marriage Fam Rev*, **35** (2016), 77–97.
32. J. Wang, Y. Xiao and Z. Peng, Modelling seasonal HFMD infections with the effects of contaminated environments in mainland China, *Appl. Math. Comput.*, **271** (2016), 615–627.
33. Y. Zhu, B. Xu, X. Lian, W. Lin, Z. Zhou and W. Wang, A hand-foot-and-mouth disease model with periodic transmission rate in Wenzhou, China, *Abstr. Appl. Anal.*, **15** (2014), 1–11.
34. Y. Li, J. Zhang and X. Zhang, Modelling and preventive measures of hand, foot and mouth disease (HFMD) in China, *Int. J. Environ. Res. Pub. Heal.*, **11** (2014), 3108–3117.
35. Y. Li, L. Wang, L. Pang and S. Liu, The data fitting and optimal control of a hand, foot and mouth disease (HFMD) model with stage structure, *Appl. Math. Comput.*, **276** (2016), 61–74.
36. J. Liu, Threshold dynamics for a HFMD epidemic model with periodic transmission rate, *Nonlinear Dynam.*, **64** (2011), 89–95.
37. J. Y. Yang, Y. Chen and F. Q. Zhang, Stability analysis and optimal control of a hand-foot-mouth disease (HFMD) model, *J. Appl. Math. Comput.*, **41** (2013), 99–117.
38. G. P. Samanta, Analysis of a delayed hand-foot-mouth disease epidemic model with pulse vaccination, *Syst. Sci. Control Eng.*, **2** (2014), 61–73.
39. R. Viriyapong and S. Wichaino, Mathematical modeling of hand, foot and mouth disease in the Northern Thailand, *Far East J. Math. Sci.*, **100** (2016), 805–820.
40. S. Sharma and G. P. Samanta, Analysis of a hand-foot-mouth disease model, *Int. J. Biomath.*, **10** (2017). Article ID: 1750016.

41. P. V. D. Driessche and J. Watmough, Reproduction numbers and sub-threshold endemic equilibria for compartmental models of disease, *Math. Biosci.*, **180** (2002), 29–48.

42. W. M. Hirsch, H. Hanisch and J. P. Gabriel, Differential equation models of some parasitic infections: methods for the study of asymptotic behavior, *Commun. Pure. Appl. Math.*, **38** (1985), 733-753.

43. X. Zhao, Uniform persistence and periodic coexistence states in infinite-dimensional periodic semiflows with applications, *Can. Appl. Math. Q.*, **3** (1995), 473–495.

44. W. Wang and X. Zhao, An epidemic model in a patchy environment, *Math. Biosci.*, **190** (2004), 97–112.

45. National Bureau of Statistics of China (NBSC), *China Demographic Yearbook of 2013, 2014, 2015, 2016, 2017*. 2018 Available from: http://www.stats.gov.cn/tjsj/ndsj/.

46. S. Marino, I. B. Hogue, C. J. Ray and D. E. Kirschner, A methodology for performing global uncertainty and sensitivity analysis in systems biology, *J. Theor. Biol.*, **254** (2008), 178–196.

47. Y. Xiao, Y. Zhou and S. Tang, *Principles of biological mathematics*, Xi'an Jiaotong University Press, 2012.

48. H. O. Hartley, A. Booker, Nonlinear Least Squares Estimation, *Ann. Math. Stat.*, **36** (1965), 638–650.

49. G. Arminger and B. O. Muthén, A Bayesian approach to nonlinear latent variable models using the Gibbs sampler and the Metropolis-Hastings algorithm, *Psychometrika*, **63** (1998), 271–300.

50. S. S. Haykin, *Neural networks and learning machines*, China Machine Press, 2009.

Appendix A

The BP neural network algorithm for estimating parameters

The parameter estimation methods for nonlinear problem that are most often used in practical applications are the nonlinear least squares estimator, Metropolis-Hastings algorithm, and so on [47]. The nonlinear least squares estimator is a parameter estimation method of nonlinear model parameters based on the criterion of error squared and minimum [48]. The Metropolis-Hastings algorithm estimates the posterior distributions of the parameters and the latent variables by using Markov chain Monte Carlo methods, which usually assumes that the sample satisfies certain probability distribution such as normal distribution, Gaussian distribution, chi-square distribution and so on [49]. Possibly due to limited by sample size, prior distribution assumptions or other constraints, the above two algorithms are used to estimate the unknown parameters of system (2.1) are not well, such as between the reported HFMD cases in mainland China and the simulation of $I(t)$ of system (2.1) in 2017, the fitting errors ER with respect to the nonlinear least squares estimator (use the Fmincon function in Matlab) and metropolis-Hastings algorithm (use the source code in [47]) are 4.03×10^{-4} and 7.46×10^{-5}, respectively, which are much larger than that of our estimated algorithm based on BP neural network (see Table 3). Because the neural network is not limited by the hypothesis of sample size and prior probability distribution, we design an algorithm based on BP neural network [50],

which is one of the most widely neural network used and highly efficient [50], to estimate unknown parameters of system (2.1).

The topology of the BP neural network is shown in Figure 10. The BP neural network consists of three layers: input layer, hidden layer and output layer. The number of nodes in the input layer, the hidden layer and the output layer are 12, 93 and 8, respectively. For simplicity, we assume that $\theta = (\theta_1, \theta_2, ..., \theta_m)^T$ denotes the vector of unknown parameters of system (2.1), where each element value must be set in reasonable interval. For example, set $\theta = (\beta_1, \beta_2, \sigma, \bar{\beta}_1, \bar{\beta}_2, \bar{\sigma}, \rho, k)$ in 2017 seen in Table 2. Let $I = (I_1, I_2, ..., I_{12})^T$ and $\hat{I} = (\hat{I}_1, \hat{I}_2, ..., \hat{I}_{12})^T$. Taking the year of 2017 as an example, the estimation algorithm is described as follows:

Step1 Generate sample data: Generate n group sample data $\theta^i = (\theta_1^i, \theta_2^i, ..., \theta_m^i)^T$, $i = 1, 2, ..., n$ by Latin hypercube sampling. Then, taking θ^i into system (2.1), we can also obtain n group numerically computed data $I^i = (I_1^i, I_2^i, ..., I_{12}^i)^T$, $i = 1, 2, ..., n$ seen in Table 2;

Step2 Use BP neural network to train data: Set $\bar{P} = (I^1, I^2, ..., I^n)$ and $\bar{T} = (\theta^1, \theta^2, ..., \theta^n)$, and each element of $\bar{P}$ and $\bar{T}$ is normalized into interval $[-1, 1]$. Then, taking $\bar{P}$ as input vector and $\bar{T}$ as output vector, a three-layers BP neural network is used to train dataset, and let N_{et} be the training completed network, which the training error is less than the setting value. The detailed process of BP neural network can be seen in [50], and its specific settings are described below;

Step3 : Estimate parameters: First, taking reported data $\hat{I} = (\hat{I}_1, \hat{I}_2, ..., \hat{I}_{12})^T$ of HFMD as the input vector into the training completed network N_{et}, we can gain a output forecast vector $\theta^* = (\theta_1^*, \theta_2^*, ..., \theta_m^*)^T$. Then, taking θ^* into system (2.1), it get the simulation of I_i . Finally, we set a small positive content $\varepsilon = 0.0001$ to estimate the error function ER (4.1). if $ER < \varepsilon$, the estimated parameters θ^* are reasonable, otherwise it goes to step 1 and reset the settings of BP neural network.

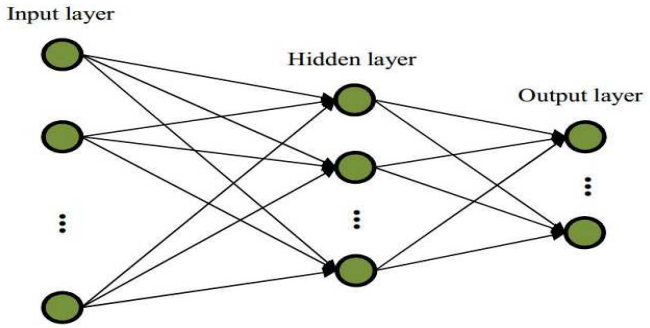

Figure 10. Structure chart of the BP neural network.

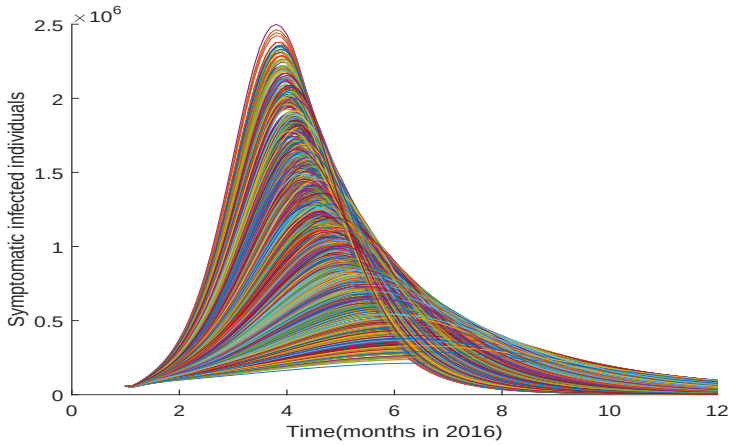

Figure 11. Multi-group numerically symptomatic infectious sample data I^i, $i = 1, 2, ..., n$ from system (2.1) in 2017, where $n = 400$. The unknown parameters $\theta = (\beta_1, \beta_2, \sigma, \bar{\beta}_1, \bar{\beta}_2, \bar{\sigma}, \rho, k)$, and the initial value and other parameter values are given in Table 2.

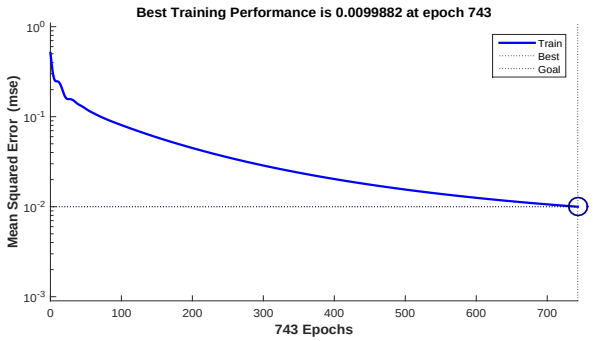

Figure 12. The neural training regression.The training goal mse is set as 0.01, and the maxmum goal epoch is set as 5000.

Figure 11 shows n group numerically computed symptomatic data I^i of system (2.1), $i = 1, 2, ..., n$, which are generated in step 1. In step 2, by using Matlab 2014b toolbox, the main settings of BP neural network are described as: (1) The transfer functions of hidden layer and output layer are tansig and purelin, respectively; (2) The network training function is trainlm; (3) The weight/bias learning function is learngdm; (4) The training error function is mse (mean squared error), and its value is 0.01; (5) The maximum iterations is 5000. Figure 12 shows the iteration process of the BP neural network, which the network complete training data before the setting maximum iterations 5000.